Analytical Biochemistry 591 (2020) 113572

Contents lists available at ScienceDirect

Analytical Biochemistry

journal homepage: www.elsevier.com/locate/yabio

Development of QCM based biosensor for the selective and sensitive detection of paraoxon

Ozan Yağmuroğlu[a,*], Sibel Emir Diltemiz[b]

[a] CBRN Department, Ministry of National Defense, Ankara, Turkey
[b] Chemistry Department, Faculty of Science, Eskisehir Technical University, 26470, Eskisehir, Turkey

ARTICLE INFO

Keywords:
Quartz crystal microbalance (QCM)
Biosensors
Electrospinning
Organophosphorus compounds
Chemical warfare agents

ABSTRACT

In this study, a quartz crystal microbalance (QCM) based sensor was developed that selectively recognizes and binds the paraoxon molecule. For this purpose, poly (styrene-maleic anhydride) (PSMA) polymer was synthesized to obtain nanofiber. A 30% (wt/wt) PSMA/DMSO solution was prepared for use in the electrospinning process, with operating conditions of 5 kV potential and 1 mL/h flow rate. After obtaining the nanofibers, AChE enzyme was immobilized to nanofiber. The QCM gold electrode surface was coated with AChE immobilized nanofiber. For this purpose, the QCM electrode was first functionalized with 4-aminothiophenol. The quartz electrode coated with the recognition layer was sequentially studied with aqueous solutions containing 50% (v/v) methanol, ranging from 0.1 ppm to 10 ppm of paraoxon. When the electrode interacts with paraoxon, the frequency value decreases. The obtained data were converted to graphs and a calibration graph was obtained. The LOD value was found to be 4.57×10^{-8} and the LOQ value was found to be 1.52×10^{-7} M. These results show us that the developed method can analyze very small quantities of paraoxon samples. The Langmuir adsorption equation was used to study the interaction of the bond between the electrode surface and the paraoxon. For the calculation of the coupling constant Ka, Δm/C (g/M) versus Δm (g) was plotted on the graph. The Ka binding constant of the obtained graphic was found to be 5×10^{7} M^{-1}

1. Introduction

Organophosphorus compounds (OPC) show their effects on the body by inhibiting nerve conduction. These compounds in general are esters, amides and phosphoric acid toluene derivatives. Organophosphates have lipid solubility. Therefore, the skin is taken up by the mucous, conjunctiva and respiratory tract. In addition, organophosphorus compounds are used as chemical agents or medicines in animal and human medicine. This group of chemicals is most commonly found in pesticides, insecticides, acaricides and so on and are readily available commercially [1,2]. The general chemical structures of organophosphorous compounds are as follows; the phosphate atom is located in the center of the molecule and the phosphate atom can double bond with oxygen or sulfur. R1-R2 in the general chemical structure represents hydrogen, alkyl (including cyclic structure), aryl, alkoxy, alkylthiol, and amino groups [3–7]. X represents halogens, cyano and thiol groups and inorganic-organic acids. The general chemical structure of the organophosphorus compounds is as shown in Fig. 1(a) [8,9].

The organophosphorous compounds show their effect on the body through the inhibition of the enzyme acetylcholine esterase. OPCs are hydrolyzed by the enzyme by binding to the serine amino acid present in the active site of the AChE (Acetylcholinesterase) enzyme. Thus, the active site of the enzyme is phosphorylated [10]. The reaction between the AChE enzyme and the OPCs takes place in two steps. First, a reversible enzyme-inhibitor complex is formed. The rate of formation of this complex depends on the structure of the organophosphorous compound, the molecular size and the alkyl groups. After formation of the recycle complex, the substitution of the alkyl group in the structure with –OH results in a non-irreversible complex. This event is called obsolescence and shown in Fig. 1(b) [11–14].

Paraoxon is an organophosphorus compound with a molecular weight of 275.2 g/mol and a closed formula of $C_{10}H_{14}NO_6P$. The chemical name is o-diethyl-o-p-nitrophenyl phosphate. The paraoxon molecule acts as an acetylcholinesterase (AChE) enzyme inhibitor in the human body. Parathion is the active metabolite of the molecule. The ability to inhibit the AChE enzyme is very strong [13]. It is one of the strongest organophosphorus compounds in terms of inhibition among insecticides. The nerve agent is 70% strong and is limited in its use as it will cause toxic effects in living organisms. Absorption by the skin is quite easy [15–17]. Paraoxon molecule structure is given in Fig. 1(c).

* Corresponding author.
E-mail addresses: ozan.yagmuroglu@msb.gov.tr (O. Yağmuroğlu), semir@eskisehir.edu.tr (S.E. Diltemiz).

https://doi.org/10.1016/j.ab.2019.113572
Received 27 September 2019; Received in revised form 19 December 2019; Accepted 29 December 2019
Available online 30 December 2019
0003-2697/

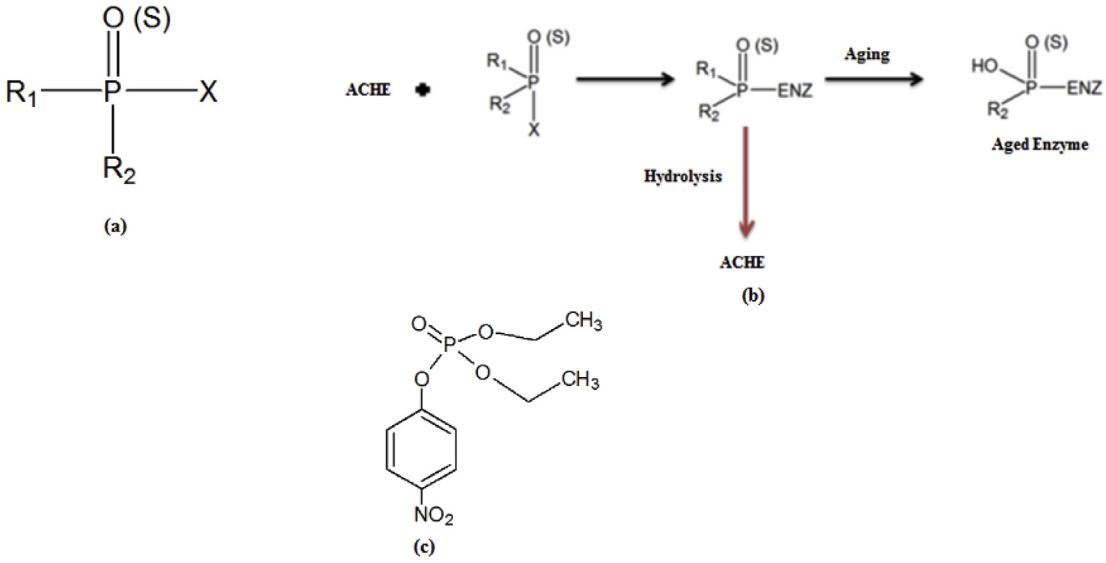

Fig. 1. (a) General chemical structure of organophosphorus compounds,**(b)** Reaction between organophosphorus compounds and AChE of organophosphorus compounds, **(c)** Chemical structure of paraoxon (O, O-diethyl-O-p-nitrophenyl phosphate).

Chemical sensors are sensor systems that convert the chemical information obtained by the concentration of the analyte in the sample into a signal. The obtained chemical information can be obtained by means of a reaction that the analyte enters the sensor surface or by the changing physical properties of the environment [14]. Chemical sensors can be classified according to the characteristics of the sensor part. There are chemical sensors that measure using only the physical changes in the environment where there is no chemical reaction. In such chemical sensors, the change of absorbance, refractive index, conductivity, temperature and mass change are measured. Measurements can be made by taking advantage of the changes in the reaction result between the analyte medium and the sensor layer [18–23]. These sensors can be called chemical sensors based on chemical primitives. A chemical sensor is a biochemical sensor in which the sensor layer is a biological molecule and the signal coming from the biochemical process is called a biochemical sensor [24–29].

Quartz crystal microbalance (QCM) is a system that uses quartz as a piezoelectric crystal and converts mass changes into electrical signals. The sensitivity of this system is very high. Usage of QCM is up to the 18th century. These devices convert very small mass changes that occur during electrochemical process to resonance frequency slip. Devices in different slip modes can be obtained by changing the cross-sectional areas of quartz crystals used in QCM. The most commonly used section is; the quartz crystal obtained by the AT-cutting method. When this crystal is obtained quartz is cut at a 350-degree angle in the Z-axis [30–36]. The surface of the electrode used in the QCM method is coated as a thin film with an analyte specific recognition layer. In this way, analysis is carried out by taking advantage of the bulk increase of the analyte which is deposited on the surface of the coated electrode. The quartz electrode used for QCM is shown in Fig. 2 [37].

Parts of QCM device; quartz electrode, oscillator and frequency counter. When an electric field is created on the QCM, oscillation in the resonance mode occurs. The susceptibility to mass change on the system is due to the frequency of vibrations occurring on the total mass of the crystal. When the resonator on the QCM device is brought into contact with the sample solution, which is connected to the electronic circuit, the change in vibration frequency occurs in parallel with the mass change. The relationship between mass and frequency change is determined by Sauerbrey equation [38].

Nanofibers; it is one of the nano-sized structures which have a threadlike appearance and are used in nanotechnology studies. They are fibers smaller than 1.0 μm in diameter. Fiber diameters are considered when nanofibers are identified. In general, the diameters of nanofibers are between 50 and 300 nm. As the fiber diameter decreases, the surface area of the unit mass decreases. Having a large surface area facilitates the immobilization of functional groups, ions and a wide variety of particles. Nanofibers are generally obtained by 5 methods. These methods can be listed as pulling, patterning, phase separation, self-assembly and electrospinning. Mechanical forces are based on methods other than electrospinning method. In the electrospinning method, an electric field is used to form the fiber from the synthesized polymer [39].

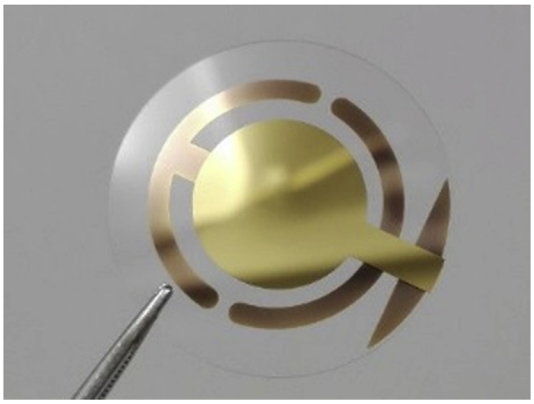

Fig. 2. Quartz crystal electrode.

Because of the ease of application in nanofiber production and the small diameters of the fibers obtained, the most effective method is electrospinning. In the production of nanofibers by electrospinning, the polymer to be used primarily is solved in a suitable solvent or dissolved by heat.

It is then placed in a pipette or injector [40] (see Fig. 3). Because of the large molecular chains present in the structure when examined nanofibers structurally, classical physics have properties that can be explained by quantum physics due to the atoms in their surface. Their surface energies, strengths and conductivities are achieved through their nano-size acquisition [41]. As fiber diameters decrease below 100 nm, the elastic modulus and mechanical strength of nanofibers increase [42]. Thanks to the electrospinning method, nanofibers with a high surface area per unit volume and very small fiber diameters can be obtained. When nanofibers are obtained, fibers with electrical

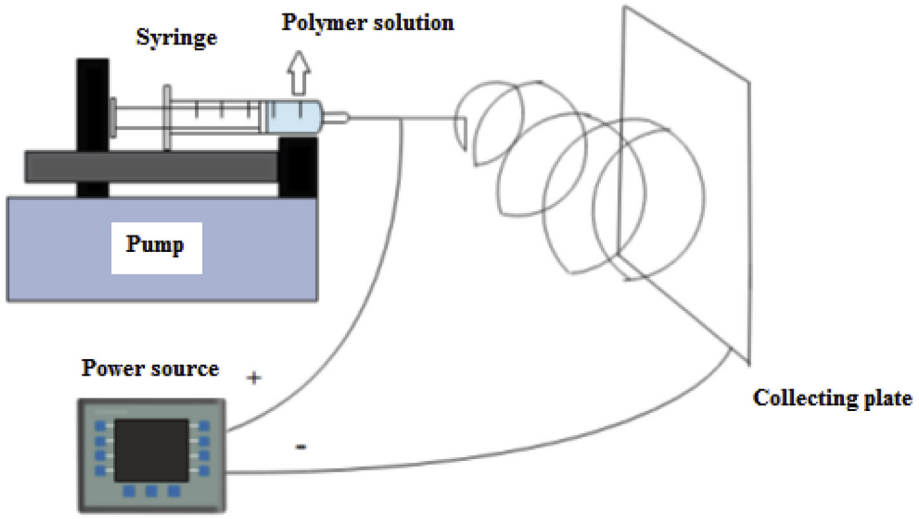

Fig. 3. Schematic representation of the electrospinning experiment setup.

conductivity at the nano-level can be obtained using conductive polymers, metals, semiconductors [43].

In this study, QCM electrode surface was coated with acetylcholinesterase (AChE) enzyme immobilized nanofiber. Due to contact of the analyte solution to electrode, the paraoxon molecules are bound to the AChE enzyme on the electrode surface. As a result of this interaction, an analysis was made using the change in mass.

2. Materials and methods

All chemicals used in the studies were taken from Sigma-Aldrich (St. Louis, USA). Thermo Scientific Barnstead™ Smart2Pure™ pure water device was used to obtain pure water. The conductivity of pure water is 18 $M\Omega cm^{-1}$.

2.1. Synthesis of poly (styrene-maleic anhydride) polymer

In this study, the method of Cecile et al.'s study was used for the synthesis of poly (styrene-maleic anhydride) (PSMA) [44]. According to this method, firstly 60 mL of toluene was taken and mixed with 3.5 mL of styrene. 2.99 g of maleic anhydride was then added to this mixture and stirred for 10 min on a magnetic stirrer. After mixing, 0.01 g of azobisisobutyronitrile (AIBN) was finally added and the mixture was stirred for 4 h at 90 °C for polymerization. During the polymerization, the reaction shown in Fig. 4 took place.

At the end of 4 h, the obtained PSMA polymer was recovered from the solution. The resulting polymer was then washed five times with toluene. After washing, the polymer was allowed to stand at room temperature for 24 h.

2.2. Preparing PSMA solutions to obtain nanofibers by electrospinning

Two different solvents were used to prepare the PSMA solution. These; dimethyl sulfoxide (DMSO) and dimethylformamide (DMF). Three different solutions of PSMA were prepared using these solvents. These; 30% (wt/wt) PSMA/DMSO, 30% (wt/wt) PSMA/DMF and 15% (wt/wt) PSMA/2.5% (wt/wt) PVA/DMSO. 40 mL of each of these solutions was prepared and 2 mL was used for each electrospinning operation.

2.3. Establishment of the electrospinning system

A direct current generating power source is used in the electrospinning process with a capacity of 30 kV. Aluminum foil cut in dimensions of 10 × 10 cm^2 was used as collecting plate to collect the formed fibers. After the solution prepared to form the fiber was drawn into the syringe, the syringe was placed in the pump assembly. The positive end of the power source is attached to the needle of the syringe. The grounded electrode is attached to the collector plate. The experiment setup is shown in Fig. 5.

2.4. Determination of operating conditions of the electrospinning system

The purpose of the electrospinning process is to obtain nanofibers on the collector plate. It is not desirable to have beaded structures in the obtained nanofiber. Therefore, the operating conditions of the system must be well defined. The distance between the syringe and the collecting plate was kept constant at 10 cm, and the applied potential and flow rate were changed. It was attempted to obtain the most suitable nanofiber by working at a potential range of 5–7 kV and a flow rate of

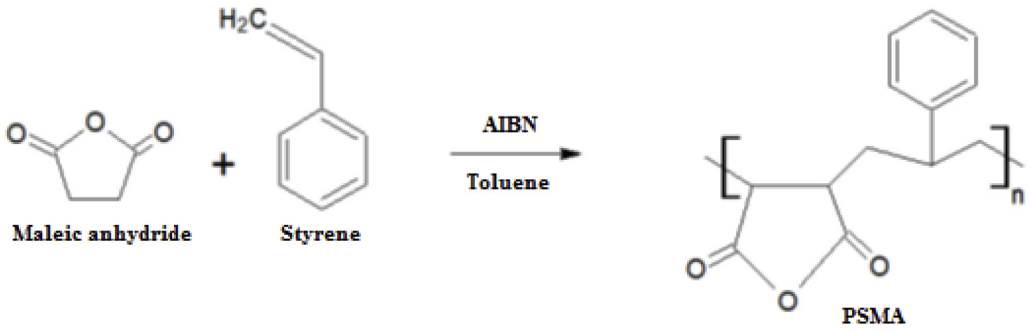

Fig. 4. Synthesis reaction of PSMA.

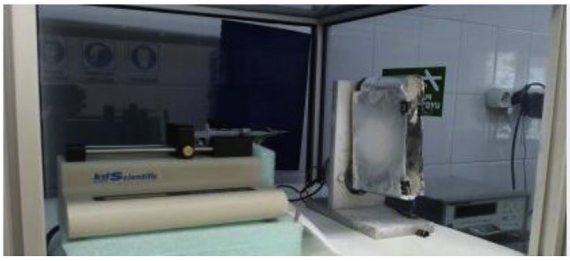

Fig. 5. Electrospinning setup in laboratory.

1–2 mL/h. The duration of the electrospinning was 10 min. The resulting nanofibers were analyzed by scanning electron microscopy (SEM) and optimum operating conditions were determined.

2.5. Cross-linking of the obtained PSMA nanofibers

Nanofibers obtained after electrospinning process; unit volume is cross-linked to increase fiber density and reduce water solubility. 1,4-Phenyldiamine was used as the crosslinker. For this, firstly 10 mL of 0.1 M Na_2CO_3/HCO_3 (pH = 9) solution was prepared. 0.7420 g of 1,4-phenyldiamine cross-linker was dissolved in 10 mL of Na_2CO_3/HCO_3. 0.25 g of nanofibers to be crosslinked were weighed and immersed in the crosslinker solution. The nanofiber solution prepared in this way was allowed to stand for 24 h at 4 °C to effect cross-linking. The cross-linking reaction of the nanofibers is shown in Fig. 6.

2.6. HRP (Horseradish Peroxidase) enzyme immobilization to cross-linked PSMA nanofibers

In order to determine the enzyme immobilization performance of the crosslinked nanofibers prepared, the HRP enzyme was first immobilized. Prior to enzyme immobilization, glutaraldehyde was used to activate cross-linked nanofibers for immobilization. For this purpose, a 10% (v/v) aqueous solution of gluteraldehyde was first prepared. 12.5 mL of this solution was taken and cross-linked nanofibers obtained from 0.25 g PSMA nanofibers were immersed in this solution. The nanofibers were thus incubated for 1 h at 4 °C. At the end of 1 h, the nanofibers were removed to remove the unreacted glutaraldehyde and placed in distilled water and allowed to stand for 2 days at 4 °C. H_2PO^{-4}/HPO_4^{2-} (pH = 7) buffer was prepared for use in HRP enzyme immobilization. 65.7 mg of HRP enzyme was dissolved in 1 ml of H_2PO^{4-}/HPO_4^{-2} buffer to obtain a stock solution. 190.2 μL of stock solution was removed and diluted to 25 mL with buffer solution. The cross-linked nanofibers were immersed in 12.5 mL of the HRP solution and incubated at 4 °C for 20 h. After enzyme immobilization, the nanofibers were reacted with TMB (Tetramethyl benzidine), the substrate of HRP enzyme.

2.7. Functionalization of quartz electrode surface

In order to bind enzyme-immobilized nanofibers to the surface of the quartz electrode, the surface of the electrode must first be functionalized. For this purpose, 4-aminothiophenol was dissolved in ethanol and 10 mL of 10 mM solution was prepared. This solution was taken into the injector. This solution in the syringe is dropped to the gold surface of the quartz electrode using a perilstaltic pump so that it is 1 mL every 30 min. This process was continued for 5 h. The schematic representation of the surface functionalization process is as shown in Fig. 7.

2.8. Creation of recognition layer at QCM electrode surface

First, 4 mL of 30 (wt/wt) PSMA/DMSO solution was prepared. 1 ml of bis (2-2′-bipyridyl) $(MATyr)_2$ ruthenium (MAT-Ru $(bipyr)_2$-MAT) was added on top of the prepared solution and stirred for 10 min at room temperature. Then, 0.38 μL of 100 ppm acetylcholinesterase enzyme was added onto the present solution. After the addition of the enzyme, the solution was stirred at room temperature for 10 min 0.5 g of ammonium persulfate was added after the end of the mixing process. The resulting final solution was allowed to stir at room temperature for 1 h. After mixing, the solution is drawn into the syringe and attached to the pump in the electrospinning device. The QCM electrode was placed on the collection plate and electrospinning was applied. A schematic representation of the processes performed is given in Fig. 8.

Then the electrode coated with the nanofiber was placed in the QCM device and its interaction with the paraoxon solution at different concentrations was investigated. For this, aqueous solutions containing 50% (v/v) methanol of paraoxon ranging from 0.1 to 10 ppm were prepared. The subsequent change in frequency of the analyte interacting with the electrode surface was measured.

3. Results

3.1. Operating conditions of the electrospinning system

In order to determine the optimal operating conditions in electrospinning process, nanofibers were obtained under different conditions and their SEM images were examined. Different solvent environments have been tested for varying flow velocities ranging from 1 to 2 mL/h to 5–7 kV. The preliminary study conditions are given in Fig. 9. These conditions were used for 30% (wt/wt) PSMA/DMSO, 30% wt/wt PSMA/DMF and 15% wt/wt PSMA/2.5% wt/wt PVA/DMSO solutions. As a result of these experiments; It is aimed to obtain homogeneous fiber diameter, non-bead structure and continuous nanofiber.

A preliminary study was conducted under conditions determined for the 30% (wt/wt) PSMA/DMSO solution. The resulting nanofibers were

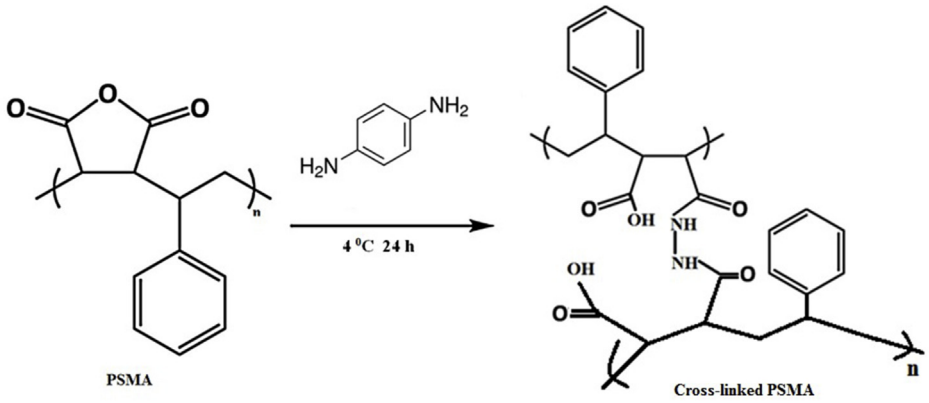

Fig. 6. PSMA cross-linking reaction.

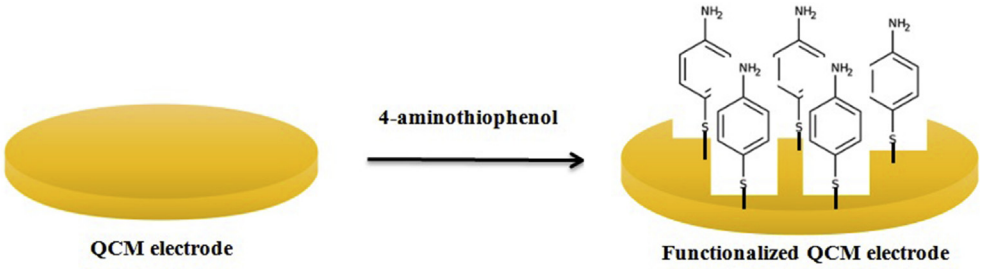

Fig. 7. Surface functionalization process.

examined at SEM. As a result, the desired nanofibers were obtained at a flow rate of 5 kV and a flow rate of 1 mL/h. It has been observed that the nanofibers obtained under other conditions are in beaded form. A SEM image of some of the nanofibers in the beaded structure is shown in Fig. 10. A SEM image of the nanofibers obtained at a flow rate of 5 kV and a flow rate of 1 mL/h is given in Fig. 11.

A preliminary study was conducted under conditions determined for the 30% (wt/wt) PSMA/DMF solution. The obtained nanofibers were examined with a SEM device. The results showed that the desired nanofibers were obtained at a flow rate of 5 kV and a flow rate of 1.5 mL/h. It has been observed that the nanofibers obtained under other conditions are in beaded form. A SEM image of some of the nanofibers in the bead structure is given in Fig. 12. A SEM image of the nanofibers obtained at a flow rate of 5 kV and a flow rate of 1.5 mL/h is given in Fig. 13.

A preliminary study was conducted under conditions determined for the 15% (wt/wt) PSMA/2.5% (wt/wt) PVA/DMSO solution. The resulting nanofibers were examined at SEM. As a result, the desired nanofibers were obtained at a flow rate of 6 kV and a flow rate of 1 mL/h. It has been observed that the nanofibers obtained under other conditions are in beaded form. A SEM image of some of the nanofibers in the beaded structure is shown in Fig. 14. A SEM image of the nanofibers obtained at a flow rate of 6 kV and a flow rate of 1 mL/h is given in Fig. 15.

When the results were examined, it was observed that 3 different solutions could obtain the nanofibers under appropriate working conditions. In order to determine the solution to be used in the study, the

(1) P: 5 kV F: 1 mL/h D: 10 cm	(2) P: 5 kV F: 1,5 mL/h D: 10 cm	(3) P: 5 kV F: 2 mL/h D: 10 cm
(4) P: 6 kV F: 1 mL/h D: 10 cm	(5) P: 6 kV F: 1,5 mL/h D: 10 cm	(6) P: 6 kV F: 2 mL/h D: 10 cm
(7) P: 7 kV F: 1 mL/h D: 10 cm	(8) P: 7 kV F: 1,5 mL/h D: 10 cm	(9) P: 7 kV F: 2 mL/h D: 10 cm

Fig. 9. Pre-study conditions.

nanofibers were compared in terms of fiber density and homogeneity. As a result of this comparison, it was decided to use the nanofibers obtained from the 30% (wt/wt) PSMA/DMSO solution at 5 kV, 1 mL/h.

3.2. Cross-linking of 30% (wt/wt) PSMA/DMSO nanofibers

The obtained nanofibers were crosslinked to increase the fiber density per unit volume and to stabilize the enzyme immobilization. How the cross-linking process is done is explained in detail in the method section. The SEM image of the cross-linked nanofibers is as

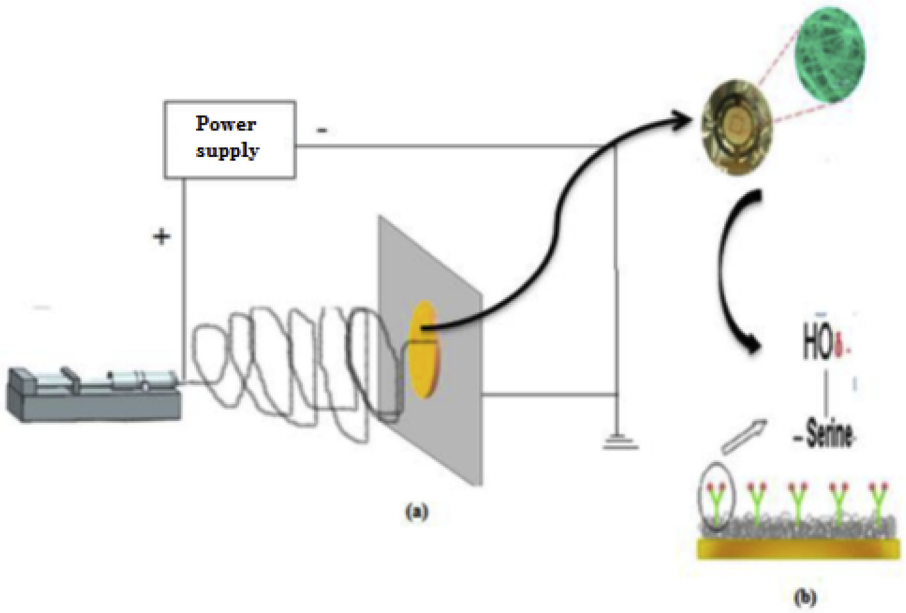

Fig. 8. Schematic of the formation of the recognition layer at the QCM electrode surface (a) electrospinning device, (b) enzyme-immobilized nanofiber-coated QCM electrode.

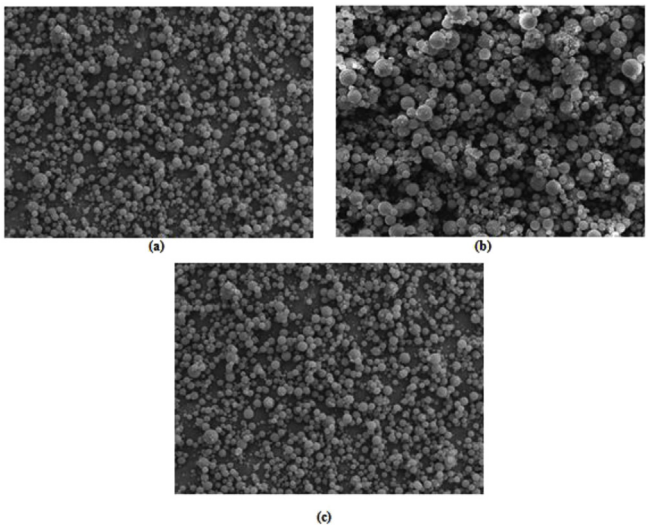

Fig. 10. The nanofibers obtained in the beaded structure from solution %30(wt/wt) PSMA/DMSO (a) 5 kV, 2 mL/h (b) 6 kV, 1 mL/h (c) 7 kV, 1,5 mL/h.

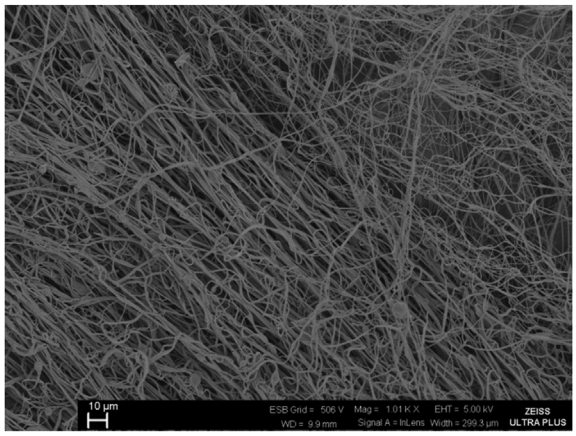

Fig. 11. The nanofiber obtained from the 30% (wt/wt) PSMA/DMSO solution without beads (5 kV, 1 mL/h).

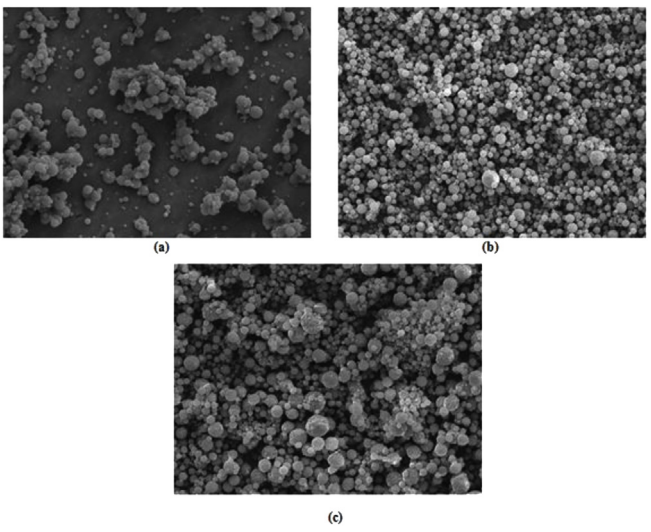

Fig. 12. The nanofibers obtained in the beaded structure from the 30% (wt/wt) PSMA/DMF solution (a) 5 kV, 1 mL/h (b) 6 kV, 1,5 mL/h (c) 7 kV, 2,0 mL/h.

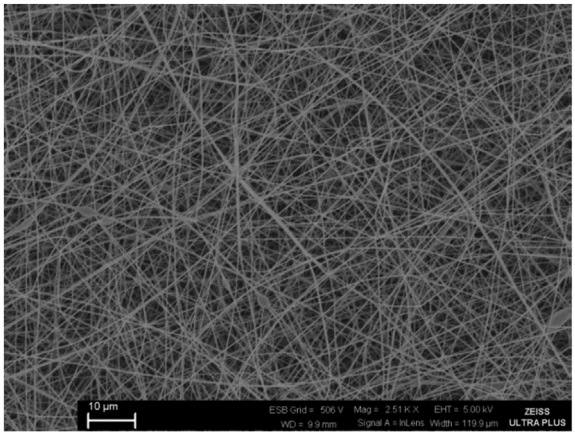

Fig. 13. The nanofiber obtained from the 30% (wt/wt) PSMA/DMF solution without beads (5 kV, 1,5 mL/h).

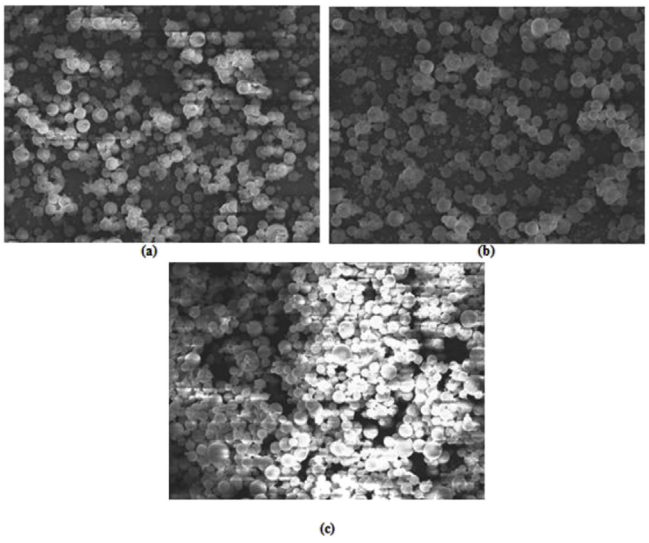

Fig. 14. The nanofibers obtained in the beaded structure from the 15% (wt/wt) PSMA/%2,5(wt/wt) PVA/DMSO nanofiller (a) 5 kV, 1,5 mL/h (b) 6 kV, 2,0 mL/h (c) 7 kV, 1,0 mL/h.

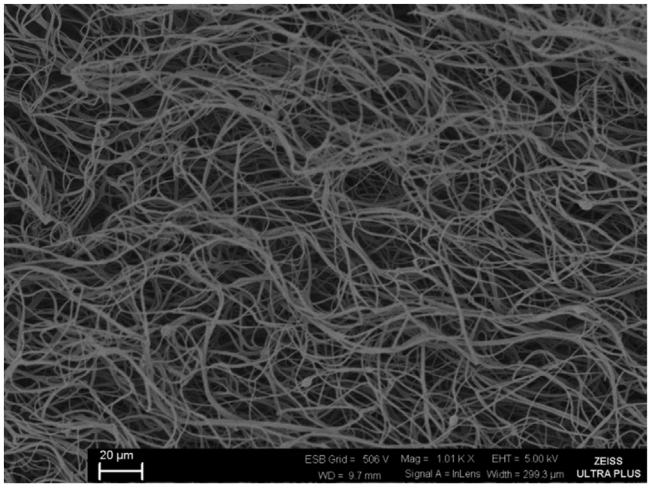

Fig. 15. The nanofiber obtained from the %15(wt/wt) PSMA/%2,5(wt/wt) solution without beads (6 kV, 1 mL/h).

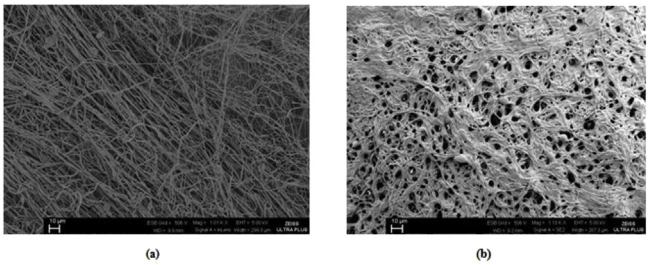

Fig. 16. Nanofibers obtained from 30% (wt/wt) PSMA/DMSO solution (a) non-crossed nanofiber (b) cross-linked nanofiber.

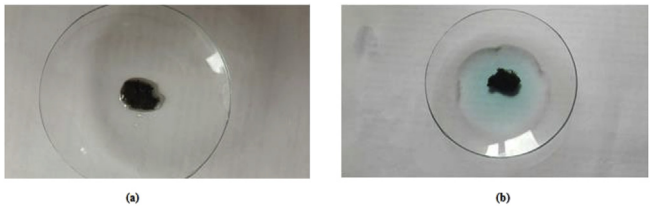

Fig. 17. Interaction with enzyme-immobilized nanofiber to substrate. (a) nanofiber not interacted with substrate (b) nanofiber interacting with substrate.

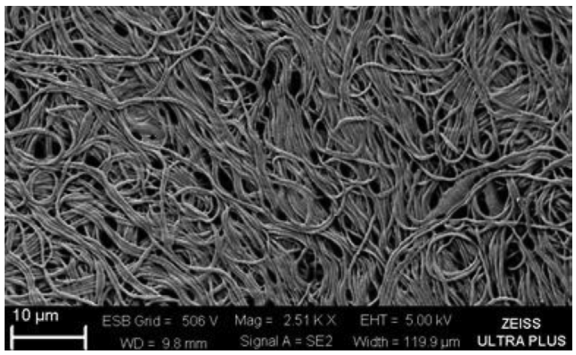

Fig. 18. Quartz crystal surface coated with nanofibers.

shown in Fig. 16.

3.3. HRP immobilization in cross-linked nanofibers

To investigate the stability of enzyme immobilization in the cross-linked nanofibers, the HRP enzyme was first immobilized. The method of immobilization of the enzyme is described in the method section. After the enzyme immobilization was performed, the nanofibers were reacted with TMB, the substrate of the HRP enzyme. After substrate addition, a color change specific to the enzyme-substrate interaction was observed. This demonstrates that immobilization of the enzyme in the nanofibers, to which we cross-link, can be carried out steadily. The interaction of the enzyme immobilized nanofibers with the substrate is shown in Fig. 17.

3.4. Coating of quartz crystal surfaces with AChE immobilized nanofiber

After the determination of the suitability of the resulting nanofibers for enzyme immobilization, the quartz crystal surface is coated with AChE immobilized nanofiber as described in the method section. Thus, the quartz crystal surface has become a recognition layer for the analyte paraoxon. The SEM image of the surface of the quartz electrode coated with nanofibers is as shown in Fig. 18.

3.5. Interaction of recognition layer-coated quartz crystal electrode with analyte

The electrode coated with nanofibers was placed in the QCM device and its interaction with the paraoxon solution at different concentrations was investigated. For this, aqueous solutions containing 50% (v/v) methanol of paraoxon ranging from 0.1 to 10 ppm were prepared. The subsequent change in frequency of the analyte interacting with the electrode surface was measured. The result of the measurement is as shown in Fig. 19.

When the electrode interacts with paraoxon, the frequency value decreases. When the concentration of the analyte is increased, the change in the negative direction in the frequency is increased. This shows that there is a mass increase on the electrode surface as a result of the bond between paraoxon and AChE. The frequency changes as a result of this mass change. Using the data obtained as a result of the measurement, the change in frequency versus concentration was plotted and a calibration graph was obtained. The drawn calibration graph is shown in Fig. 20.

The regression coefficient obtained as a result of the calibration line was found to be 0.9428. Then the amount of paraoxon adsorbed to the electrode surface was calculated as µg/cm^2 using the Sauerbrey equation. The calculated value is plotted against the paraoxon concentration. The resulting graph is as shown in Fig. 21.

The Langmuir adsorption isotherm was used to study the interaction of the bond between the electrode surface and the paraoxon. In order to calculate the Ka value, Δm/C (g/M) versus Δm (g) was plotted on the

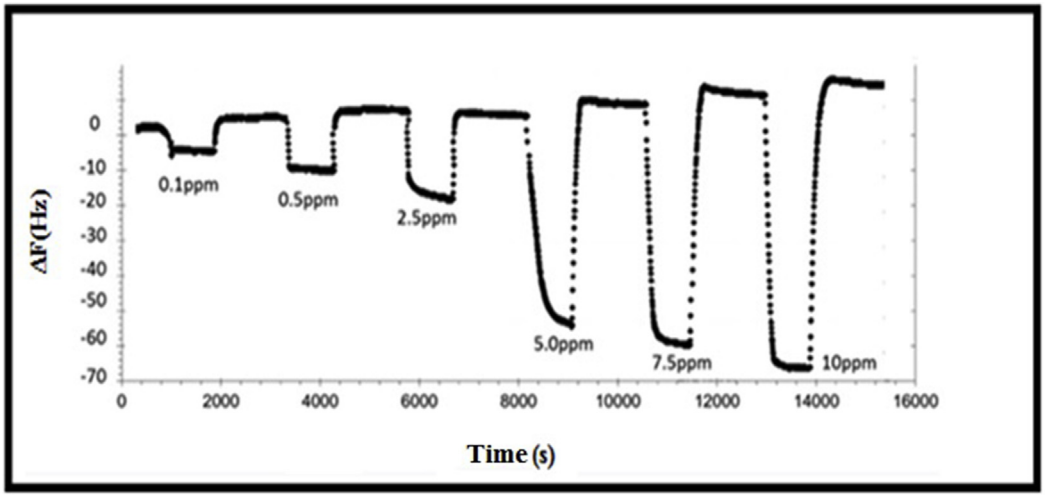

Fig. 19. Frequency change resulting from interaction of quartz crystal electrode with paraoxon.

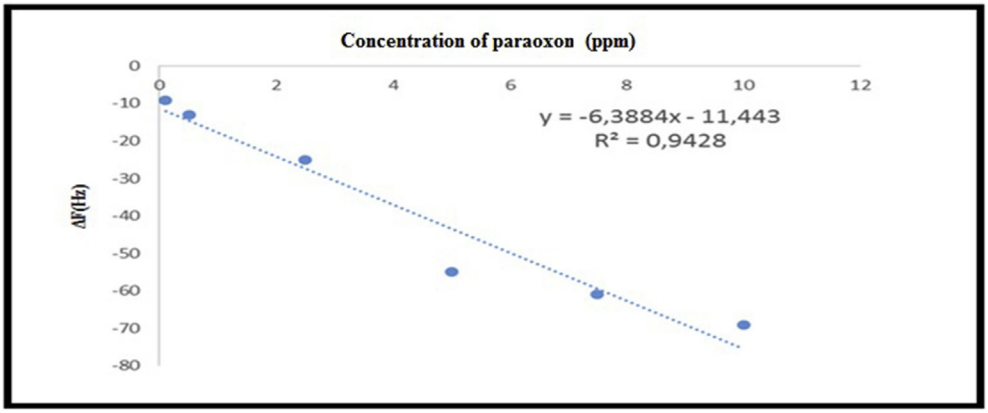

Fig. 20. Calibration chart of paraoxon samples at different concentrations in QCM biosensor.

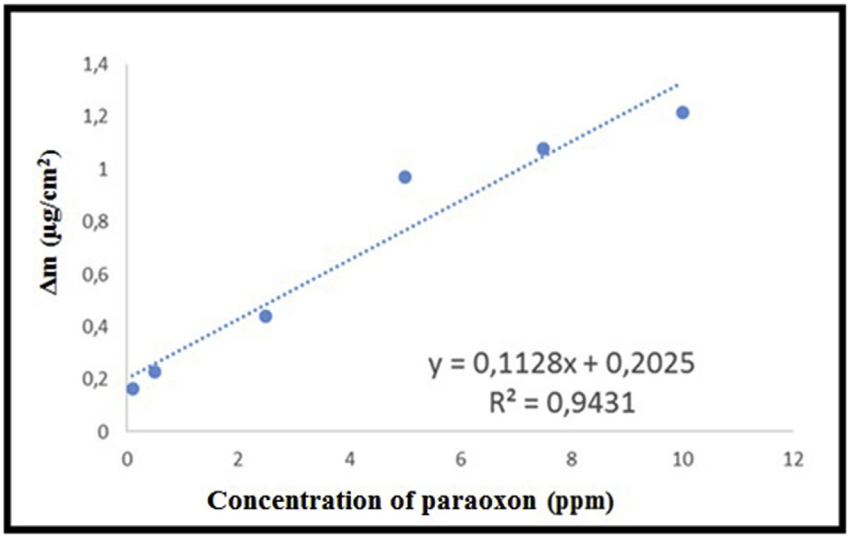

Fig. 21. Change graph of concentration of analyte versus mass change on electrode surface.

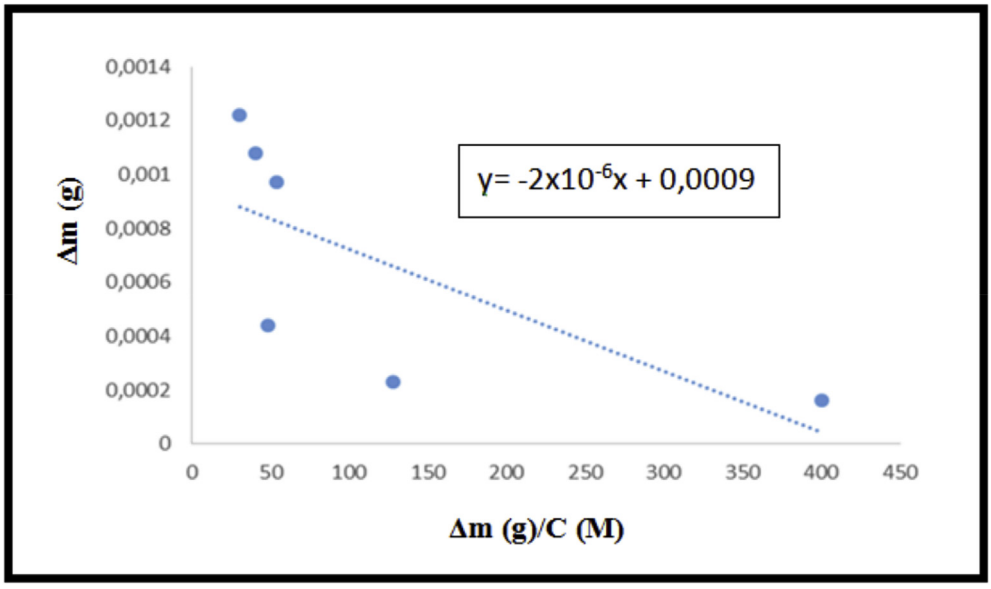

Fig. 22. Change graph of concentration of analyte versus mass change on electrode surface.

Table 1
Solutions prepared to examine the interference effect.

Paraoxon		Parathion		Ratio
ppm	mL	ppm	mL	
2	1	2	1	1:1
2	1	10	1	1:5
2	1	20	1	1:10

Table 2
Comparison of different methods with our sensor.

Method	LOD ($molL^{-1}$)
Sensor based on pH change [49]	2×10^{-6}
Amperometric proton selective sensor [50]	5×10^{-5}
Organophosphorus hydrolase enzyme immobilized glassy carbon electrode based sensor [51]	4×10^{-7}
Amperometric sensor based on carbon paste electrode [52]	1×10^{-4}
QCM	$4{,}57 \times 10^{-8}$

graph. The resulting graph is shown in Fig. 22.

The Langmuir binding constant was calculated from the equation obtained by drawing the graph. Accordingly, the Langmuir binding constant was found to be $5 \times 10^{7}\ M^{-1}$. Blank solutions were prepared for the calculation of LOD and LOQ and 5 different measurements were taken. The mean of the measurement results was 0.0646 and the standard deviation was 4.203×10^{-3}. LOD and LOQ values were used by using the standard deviation. As a result of the calculations made, the LOD value was found to be 0.0126 ppm ($4.57 \times 10^{-8}\ molL^{-1}$) and the LOQ value was found to be 0.0418 ppm ($1.52 \times 10^{-7}\ molL^{-1}$) M.

3.6. Interference effect

After the measurement of the selectivity, the performance of the developed paraoxon selective QCM based sensor under interference effect was investigated. Phenmedipham is a herbicide. ACHE enzyme and organophosphorus compounds show enzyme-substrate interaction. Phenmedipham was preferred because its molecular structure did not belong to the organophosphorus group. For this purpose, different solutions of paraoxon and phenmedipham have been prepared. Prepared solutions were given in Table 1.

The interference effect; 0.36% for 1: 1 ratio, 3.75% for 1: 5 ratio and 6.18% for 1:10 ratio were calculated respectively. From these results, it can be concluded that the interference effect of the analysis environment containing molecules similar to the chemical structure of paraoxon is negligible.

4. Conclusions

In this study, QCM biosensor for paraoxon determination was developed. For this purpose, poly (styrene-maleic anhydride) polymer was synthesized in order to obtain nanofibers. 30% (wt/wt) PSMA/DMSO was prepared as the polymer solution. Nanofibers were obtained at 5 kV potential and 1 mL/h operating conditions. To understand the suitability of the obtained nanofiber for enzyme immobilization, HRP enzyme immobilization was first performed. To check if enzyme immobilization has occurred, the enzyme was immobilized on nanofibers, interacted with TMB, the substrate of HRP, and this interaction-specific color change was observed.

After the determination of suitability for nanofiber immobilization, the quartz electrode was switched to the step of coating with the AChE enzyme immobilized nanofiber. The quartz electrode coated with the recognition layer was sequentially activated with aqueous solutions containing 50% (v/v) methanol, ranging from 0.1 ppm to 10 ppm of paraoxon. When the electrode interacts with paraoxon, the frequency value decreases. When the concentration of the analyte is increased, the change in the negative direction in the frequency is increased.

This shows that there is a mass increase on the electrode surface as a result of binding between paraoxone and acetylcholinesterase. The obtained data were converted to graphs and a calibration graph was obtained. The detection limit of the we developed sensor is $4{,}57 \times 10^{-8}\ mol\ L^{-1}$. The Langmuir adsorption equation was used to study the interaction of the bond between the electrode surface and the paraoxon.

The Ka binding constant was found to be 5×10^{7} M-1. The detection limit of the techniques that detect paraoxon with different methods is compared with the detection limit of the sensor we have developed [45–48]. The detection limit of the QCM based sensor we have developed is one of the lowest values. In addition, the sensor we have developed can be used to analyze real samples, as response time and performance are very good.

In order to evaluate the performance of the developed sensors, the literature is examined. Hydrolysis of organophosphates has been utilized in the majority of the studies in the literature and the resulting changes have been the basis of the analysis. Some of the sensors developed in the literature and the QCM based sensor are listed in Table 2 for comparison purposes.

When Table 2 is examined, it is seen that the samples containing much lower amounts of paraoxone can be analyzed with the QCM based sensor we developed.

Declaration of competing interest

The authors declare that they have no known competing financial interests or personal relationships that could have appeared to influence the work reported in this paper.

References

[1] J. Jeyeratnam, Pesticides: poisoning as a global health problem, World Health Stat. 43 (1990) 139–144.
[2] R. Kamanyire, L. Karalliedde, Organophosphate toxicity and occupational exposure, Occup. Med. (Lond.) 54 (2004) 69–75.
[3] V.K. Gupta, A. Nayak, S. Agarwal, S. Barkha, Recent advances on potentiometric membrane sensors for pharmaceutical analysis, Comb. Chem. High Throughput Screen. 14 (4) (2011) 284–302.
[4] V.K. Gupta, B. Sethi, R.A. Sharma, S. Agarwal, A. Bharti, Mercury selective potentiometric sensor based on low rim functionalized thiacalix [4]-arene as a cationic receptor, J. Mol. Liq. 177 (2013) 114–118.
[5] V.K. Gupta, M.R. Ganjali, P. Norouzi, H. Khani, A. Nayak, S. Agarwal, Electrochemical analysis of some toxic metals by ion–selective electrodes, Crit. Rev. Anal. Chem. 41 (2011) 282–313.
[6] V.K. Gupta, K.S. Suresh, J. Suresh, Determination of lead using a poly(vinyl chloride)-based crown ether membrane, Analyst 120 (1995) 495–498.
[7] V.K. Gupta, K.S. Suresh, K. Mithalesh, K. Dwivedi, Suresh, Caesium PVC–crown (dibenzo-24-crown-8) based membrane sensor, Anal. Proc. Anal. Commun. 32 (1995) 21–23.
[8] T. Karayılanoğlu, Medical Defense in Chemical Attack, third ed., GATA Basımevi, Ankara, Turkey, 2003.
[9] D.I. Dragonov, B.N. Ladu, Pharmacogenetics of paraoxonases: a brief review, Naunyn-Schmiedeberg's Arch. Pharmacol. 369 (1) (2004) 78–88.
[10] J. Bajgar, Organophosphates/Nevre Agents poisoning: mechanism of action, diagnosis, prophylaxis and treatment, Adv. Clin. Chem. 38 (2004) 152–153.
[11] J. Patocka, K. Kuča, D. Jun, Acetylcholinesterase and butyrylcholinesterase – important enzymes of human body, Acta Med. 47 (4) (2004).
[12] G. Başkol, K. Köse, Paraoksonaz: Biyokimyasal özellikleri, fonksiyonları ve klinik önemi, Erciyes Tip. Derg. (Erciyes Med. J.) 26 (2) (2004) 75–80.
[13] A.A. Kousba, L.G. Sultatos, T.S. Poe, C. Timchalk, Comparison of chlorpyrifos-oxon and paraoxon acetylcholinesterase inhibition dynamics: potential role of a peripheral binding site, Toxicol. Sci. 80 (2) (2004) 239–248.
[14] J. Stetter, W. Penrose, Understanding chemical sensors and chemical sensors arrays; past, present and future, Sens. Update 10 (2002) 189–229.
[15] V.K. Gupta, K.M. Hassan, S. Roya, Simultaneous determination of hydroxylamine, phenol and sulfite in water and waste water samples using a voltammetric nanosensor, Int. J. Electrochem. Sci. 10 (2015) 303–316.
[16] V.K. Gupta, A.K. Singh, L.K. Kumawat, Thiazole Schiff base turn-on fluorescent chemosensor for Al3+ ion, Sens. Actuators B195 (2014) 98–108.
[17] V.K. Gupta, K.S. Srivastava, S. Jain, PVC-based 2,2,2-cryptand sensor for zinc ions, Anal. Chem. 68 (1996) 1272–1275.
[18] F. Dondurmacıoğlu, Development of Optical Sensors for the Determination of

Heavy Metal Ions, Doctoral thesis İstanbul University, İstanbul, Turkey, 2011.
[19] V.K. Gupta, L.P. Singh, R. Singh, N. Upadhyay, S. Kaur, B. Sethi, A novel copper (II) selective sensor based on Dimethyl 4, 4′ (o-phenylene) bis(3-thioallophanate) in PVC matrix, J. Mol. Liq. 174 (2011) 11–16.
[20] V.K. Gupta, K.S. Ashok, L.K. Kumawat, Thiazole Schiff base turn-on fluorescent chemosensor for Al3+ ion, Sens. Actuators B Chem. 195 (2014) 98–108.
[21] V.K. Gupta, S. Kumar, L.P. Singh, B. Sethi, Cadmium (II) ion sensing through p-tert-butyl calix[6]arene based potentiometric sensor, J. Mol. Liq. 195 (2014) 65–68.
[22] V.K. Gupta, S. Karthikeyan, R. Boopathy, A. Titus, G. Sekaran, A new approach for the degradation of high concentration of aromatic amine by heterocatalytic Fenton oxidation: kinetic and spectroscopic studies, J. Mol. Liquids 173 (2012) 153–163.
[23] M.H. Dehghani, D. Sanaei, I. Ali, A. Bhatnagar, Removal of chromium(VI) from aqueous solution using treated waste newspaper as a low-cost adsorbent: kinetic modeling and isotherm studies, J. Mol. Liq. 215 (2016) 671–679.
[24] A. Hulanicki, S. Glab, F. İngman, Chemical sensors definitions and classification, Pure Appl. Chem. 63 (9) (1991) 1247–1250.
[25] A. Asfaram, M. Ghaedi, S. Agarwal, I. Tyagi, V.K. Gupta, Removal of basic dye Auramine-O by ZnS:Cu nanoparticles loaded on activated carbon: optimization of parameters using response surface methodology with central composite design, RSC Adv. 5 (2015) 18438–18450.
[26] V.K. Gupta, N. Atar, M.Y. Yola, Z. Üstündağ, L. Uzun, A novel magnetic Fe@Au core–shell nanoparticles anchored graphene oxide recyclable nanocatalyst for the reduction of nitrophenol compounds, Water Res. 48 (2014) 210–217.
[27] M.L. Yola, V.K. Gupta, T. Eren, A.E. Şen, N. Atar, A novel electro analytical nanosensor based on graphene oxide/silver nanoparticles for simultaneous determination of quercetin and morin, Electrochim. Acta 120 (2014) 204–211.
[28] M.L. Yola, V.K. Gupta, T. Eren, A.E. Şen, N. Atar, A novel electro analytical nanosensor based on graphene oxide/silver nanoparticles for simultaneous determination of quercetin and morin, Electrochim. Acta 120 (2014) 204–211.
[29] V.K. Gupta, N. Mergu, K. Kumawat, A.K. Singh, Selective naked-eye detection of Magnesium (II) ions using a coumarin-derived fluorescent probe, Sens. Actuators B. 207 (2015) 216–223.
[30] S. Diltemiz, Development of a biosensor based on molecularly imprinted polymer techniques with DNA recognition sites, Doctoral Thesis, Anadolu Üniversitesi, Eskişehir, Turkey, 2006.
[31] A. Shons, F. Dorman, J. Najarian, The piezoelectric Quartz immunosensor, J. Biomed. Mater. Res. (1972) 570–576.
[32] K.D. Pavey, Quartz crystal analytical sensors: the future of label-free, real-tim diagnostics, Expert Rev. Mol. Diagn. 2 (2002) 173–286.
[33] V.K. Gupta, N. Mergu, K. Kumawat, A.K. Singh, A reversible fluorescence “off–-on–off” sensor for sequential detection of aluminum and acetate/fluoride ions, Talanta 144 (2015) 80–89.
[34] V.K. Gupta, H. Karimi-Maleh, F. Tahernejad-Javazmi, N. Atar, M.L. Yola, A.A. Ensafi, A novel DNA biosensor based on a pencil graphite electrode modified with polypyrrole/functionalized multiwalled carbon nanotubes for determination of 6-mercaptopurine anticancer drug, Ind. Eng. Chem. Res. 54 (2015) 3634–3639.
[35] V.K. Gupta, P. Kumar, Cadmium(II)-selective sensors based on dibenzo-24-crown-8 in PVC matrix, Anal. Chim. Acta 389 (1999) 205–212.
[36] V.K. Gupta, A. Jain, B.B. Sahoo, L.P. Singh, Neutral carrier and organic resin based membranes as sensors for uranyl ions, Anal. Proc. Anal. Commun. 32 (1995) 263–265.
[37] D. Çökeliler, Preparation of Mass-Sensitive Immunosensors by the Plasma Polymerization Method for the Determination of Alphatoxin, Doctoral thesis, Hacettepe Üniversitesi, Ankara, Turkey, 2006.
[38] R.D. Vaughan, C.K. O'Sullivan, G.G. Guilbault, Sulfur based self assembled monolayers (SAM's) on piezoelectric crystals for immunosensor development, Fresenius J. Anal. Chem. 364 (1999) 54–57.
[39] F. Audrey, I.S. Chronakis, Polymer nanofibers assembled by electrospinning, Curr. Opin. Colloid Interface Sci. 8 (2003) 64.
[40] G.C. Rutledge, S.V. Fridrikh, Formation of fibers by electrospinning, Adv. Drug Deliv. Rev. 59 (2007) 1384–1391.
[41] D. Rodoplu, Modification of Quartz Crystal Micro-scale Surfaces by Electro-Spinning Method for Biosensor Applications, Master thesis Hacettepe Üniversitesi, Ankara, Turkey, 2011.
[42] J. He, L. Xu, Y. Wu, Y. Liu, A mathematical models for continuous electrospun nanofibers and electrospun nanoporous microspheres, Polym. Int. 56 (2007) 1323–1329.
[43] S. Agarwal, J.H. Wendorff, A. Greiner, Use of electrospinning technique for biomedical applications, Polymer 49 (2008) 5603–5621.
[44] C. Cecile, Y.L. Hsieh, Hydrophilic polystyrene/maleic anhydride ultrafine fibrous membranes, J. Appl. Polym. Sci. 115 (2009) 723–730.
[45] J. Wang, R. Krause, K. Block, M. Musameh, A. Mulchandani, Dual amperometric-potentiometric biosensor detection system for monitoring organophosphorus neurotoxins, Anal. Chem. Acta 469 (2009) 197–203.
[46] M. Hossain, M. Faisal, C. Kim, H. Cha, S. Nam, J. Lee, Amperometric proton selective strip-sensors with a microelliptic liquid/gel interface for organophosphate neurotoxins, Electrochem. Commun. 13 (2011) 611–614.
[47] C. Lei, M.M. Valenta, K.P. Saripalli, E.J. Ackerman, Biosensing paraoxon in simulated environmental samples by immobilized organophosphorus hydrolase in functionalized mesoporous silica, J. Environ. Qual. 36 (2007) 233–238.
[48] Z. Meng, T. Yamazaki, K. Sode, Enhancement of the catalytic activity of an artificial phosphotriesterase using a molecular impirinting technique, Biotechnol. Lett. 25 (2003) 1075–1080.
[49] J. Wang, R. Krause, K. Block, M. Musameh, A. Mulchandani, Dual amperometric-potentiometric biosensor detection system for monitoring organophosphorus neurotoxins, Anal. Chem. Acta 469 (2009) 197–203.
[50] M. Hossain, M. Faisal, C. Kim, H. Cha, S. Nam, J. Lee, Amperometric proton selective strip-sensors with a microelliptic liquid/gel interface for organophosphate neurotoxins, Electrochem. Commun. 13 (2011) 611–614.
[51] C. Lei, M.M. Valenta, K.P. Saripalli, E.J. Ackerman, Biosensing paraoxon in simulated environmental samples by immobilized organophosphorus hydrolase in functionalized mesoporous silica, J. Environ. Qual. 36 (2007) 233–238.
[52] Z. Meng, T. Yamazaki ve K. Sode, Enhancement of the catalytic activity of an artificial phosphotriesterase using a molecular impirinting technique, Biotechnol. Lett. 25 (2003) 1075–1080.